Ballistic electron emission microscopy spectroscopy study of AlSb and InAs/AlSb superlattice barriers*

X.-C. Cheng and T. C. McGill
Department of Applied Physics, California Institute of Technology, Pasadena, California 91125

(Received 21 January 1998; accepted 28 May 1998)

Due to its large band gap, AlSb is often used as a barrier in antimonide heterostructure devices. However, its transport characteristics are not totally clear. We have employed ballistic electron emission microscopy (BEEM) to directly probe AlSb barriers as well as more complicated structures such as selectively doped *n*-type InAs/AlSb superlattices. The aforementioned structures were grown by molecular beam epitaxy on GaSb substrates. A 100 Å InAs or 50 Å GaSb capping layer was used to prevent surface oxidation from *ex situ* processing. Different substrate and capping layer combinations were explored to suppress background current and maximize transport of BEEM current. The samples were finished with a sputter deposited 100 Å metal layer so that the final BEEM structure was of the form of a metal/capping layer/semiconductor. Of note is that we have found that hole current contributed significantly to BEEM noise due to type II band alignment in the antimonide system. BEEM data revealed that the electron barrier height of Al/AlSb centered around 1.17 eV, which was attributed to transport through the conduction band minimum near the AlSb *X* point. Variation in the BEEM threshold indicated unevenness at the Al/AlSb interface. The metal on semiconductor barrier height was too low for the superlattice to allow consistent probing by BEEM spectroscopy. However, the superlattice BEEM signal was elevated above the background noise after repeated stressing of the metal surface. A BEEM threshold of 0.8 eV was observed for the Au/24 Å period superlattice system after the stress treatment. [S0734-211X(98)12004-8]

I. INTRODUCTION

There has been much interest in the GaSb, AlSb, and InAs lattice matched material system. Due to the unique type II band alignment and narrow band gaps of these materials, much research has focused on developing antimonides for infrared lasers[1,2] and detectors,[3] as well as for high speed integrated circuits.[4] Common to all these devices is the need for a barrier like constituent such as AlSb. However, AlSb barriers often appear leaky, especially in Schottky gate type applications.[5,6] Moreover, AlSb is *p* type when left unintentionally doped, and *n*-type doping of AlSb is not always convenient. Recently, it has been reported that InAs/AlSb superlattices can be an attractive alternative for *n*-type barrier applications such as making cladding layers in laser structures.[7] The superlattice approximately lattice matches with GaSb when the InAs and AlSb constituent layers are given the same thickness. The band gap and effective barrier height of the superlattice are tunable by varying the superlattice period, and *N*-type doping can be achieved by incorporating Si in the InAs well.

In this article, ballistic electron emission microscopy (BEEM) was used to characterize these antimonide barrier structures. BEEM is a technique based on scanning tunneling microscopy (STM) and is especially suited to study of local transport properties.[8,9] In a BEEM experiment, the semiconductor of interest is coated with a thin layer of metal, which supports STM tunnel current while a collector terminal at the back of the sample conducts away electrons that leak across the metal–semiconductor interface. In BEEM spectroscopy, the collector current is monitored as a function of tunneling voltage while the tunneling current is kept constant by varying the STM tip to sample distance. As the STM tip potential rises above the bottom of the semiconductor conduction band, electrons can travel ballistically across the thin metal region and enter the semiconductor unimpeded, causing a noticeable increase in collector current. Thus the BEEM turn on threshold depends on the underlying semiconductor band structure and can be used to evaluate Schottky barrier heights and semiconductor band edges in the antimonide material system. The scanning probe nature of BEEM allows local variations of these properties to be mapped and was utilized to examine the integrity of AlSb barriers.

Since its inception, BEEM spectroscopy has been used extensively to study metal on semiconductor structures. It has been adapted by several workers to study the Au/Si (Ref. 9) and the $Au/Al_xGa_{1-x}As$ system.[10,11] Recently, the technique has been successfully applied to GaAs/AlAs (Ref. 12) and InAs/AlSb (Ref. 13) double barrier heterostructures, which indicates that the technique is promising for probing less conventional systems such as the aforementioned InAs/AlSb superlattice.

II. EXPERIMENT

The samples used in this experiment were grown in a Perkin–Elmer 430 molecular beam epitaxy (MBE) system equipped with a valved As cracker. Figure 1 shows the structure of typical BEEM samples. Te doped ($n=5\times10^{17}$ cm^{-3}) GaSb wafers were used for most of the growth. This was to ensure that the substrate would be conductive enough in subsequent BEEM experiments. Follow-

*No proof corrections received from author prior to publication.

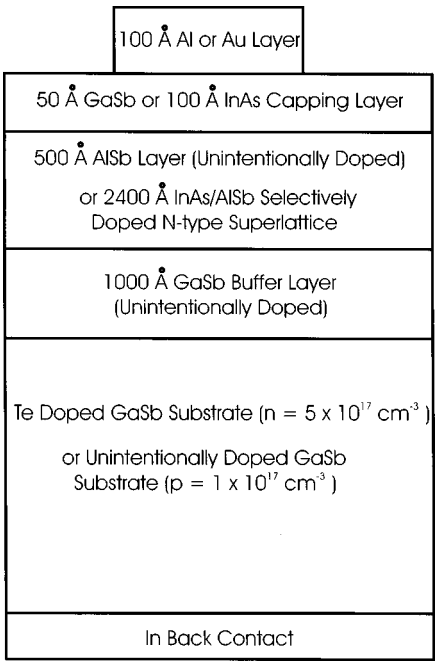

FIG. 1. Structure of the BEEM samples.

ing oxide desorption under Sb overpressure, an unintentionally doped GaSb buffer layer was grown. Since GaSb is *p* type from background doping, the buffer layer was kept as thin as possible without compromising the structural quality of subsequent growth. At low growth rate, a 1000 Å thick buffer layer was found to be adequate. At the end of the buffer growth, samples were soaked in Sb, yielding the (1 $\times$3) reflection high energy electron diffraction (RHEED) pattern characteristic of a reconstructed GaSb surface.

For AlSb studies, a 500 Å layer of unintentionally doped AlSb was grown over the smoothed GaSb surface. The thickness was selected so that the bulk properties could be examined while at the same time the layer was thin enough to support transport of BEEM current. Because the AlSb layer was relatively thin, the substrate temperature was kept at 520 °C, the same as for GaSb growth. RHEED for the AlSb layer was less streaky but still showed the characteristic 1 $\times$3 pattern. To prevent AlSb oxidation, the samples were capped off at the end of the growth by either a 50 Å GaSb layer or a 100 Å InAs layer. The substrate temperature was lowered to 470 °C for growing the InAs capping layer.

For growth of the selectively doped InAs/AlSb superlattice, the substrate temperature had to be lowered to prevent excessive As incorporation in the antimonide layers. The structural quality of the superlattice was significantly improved when the growth temperature was lowered to 420 °C, at which point the GaSb surface turns Sb rich and the RHEED pattern changes from 1$\times$3 to 1$\times$5. During growth of the InAs constituent layer, the Si dopant cell shutter was opened, and As flux was minimized by using the valved cracker while maintaining an As stabilized growth front. A 10 s Sb soak was applied between each InAs and AlSb interface to ensure a InSb like interface, which is known to produce material of superior quality.[14] The RHEED pattern remained streaky throughout the growth and exhibited sharp 2$\times$4 and 1$\times$3 reconstructions for the InAs and AlSb layers, respectively. The samples were grown with superlattice periods of 17, 24, and 48 Å. The period thickness was split between the InAs and AlSb layers, which were under alternative compressive and tensile strain. The total thickness of the superlattice was kept constant for all the samples at 2400 Å. To prevent oxidation, the superlattice was capped with 50 Å of GaSb following completion of the last AlSb layer.

A sputter-etch deposition system was used for postgrowth metallization. Aluminum and gold were sputtered off solid targets by Ar plasma and deposited onto the sample at rates up to 0.4 Å/s. The samples were placed behind a mask and patterned with arrays of metal dots 1 mm^2 in area. Metal layer thicknesses up to 100 Å were experimented. Atomic force microscopy (AFM) studies showed that the typical metal layer had a root mean square (rms) roughness on the order of 5 Å. For most samples, the surface morphology was smooth and appeared suitable for BEEM studies. Prior to metallization, samples were taken out of the ultrahigh vacuum (UHV) growth environment and exposed to the ambient. Hence a 20–30 Å thick native oxide was present between the metal and semiconductor layer. Talin *et al.* have shown that the oxide layer does not affect BEEM results for Au/GaAs structures.[15] In our study, it was found that the antimonide samples with native oxides were stable for up to several weeks. To minimize contamination from handling, a degreasing procedure was followed before the sample was introduced to the metallization chamber which may partially remove the native oxide layer. It consisted of sequential ultrasonic rinses in acetone, isopropanol, and de-ionized water, with each rinse lasting 2 min. The procedure helped generate more consistent BEEM results, especially for the samples that have been stored in air for some time.

Our BEEM setup was configured for experiments in air at room temperature. It was based on a Digital Instruments scanning tunneling microscope unit (Nanoscope III). A fine Au wire was spring mounted against the top of the sample as the STM base contact, while indium left from the growth, on the back side of the sample, served as the BEEM back contact. The setup was tested and calibrated with the Au/Si(100) system. The equipment has also been successfully used to study the $Au/Al_xGa_{1-x}As$ system.[11]

III. RESULTS AND DISCUSSION

Prior to BEEM experiments, samples were characterized by $I-V$ measurements. Figure 2 shows the results from two types of AlSb samples. Sample A was from an early growth on an unintentionally doped *p*-type GaSb substrate and capped by an InAs layer. Sample B was grown on an *n*-type GaSb substrate and capped by GaSb. The sample B substrate/capping layer combination was standard for most of the AlSb samples and for all superlattice samples. As can be seen from the $I-V$ behavior of sample A, AlSb acted as a poor barrier for the InAs/GaSb junction, which allowed holes to tunnel out of the underlying *p*-type substrate, raising the

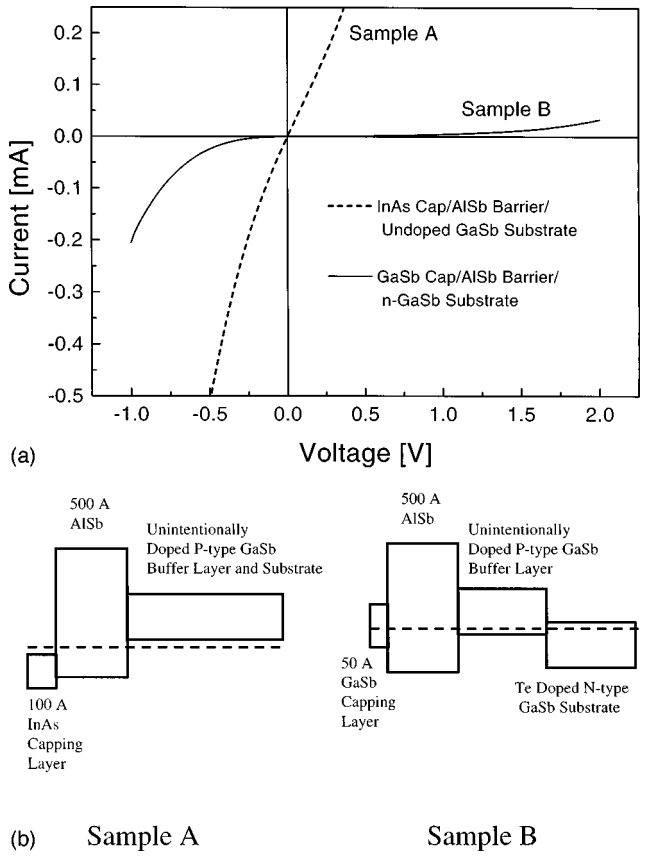

FIG. 2. $I-V$ curves (a) and flat band diagrams (b) for two types of AlSb BEEM samples. Both samples were metallized with 100 Å of Al. The Al mesa had an area of 1 mm^2. Sample B yielded BEEM curves but sample A was too noisy for BEEM measurements.

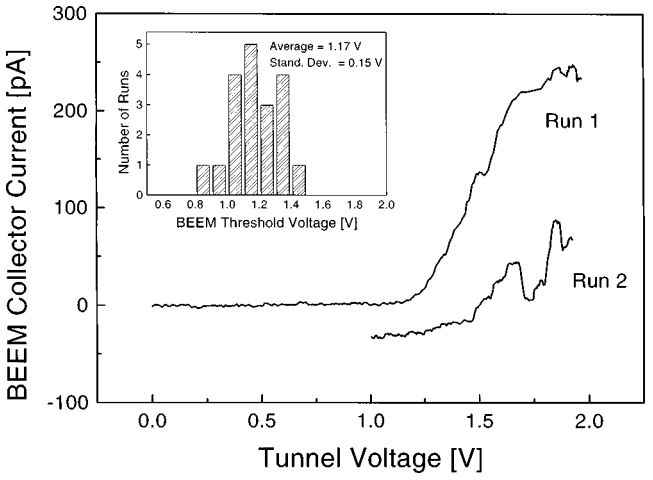

FIG. 3. BEEM $I-V$ curves for AlSb barriers grown on n-type GaSb substrates. The samples were capped with 50 Å of GaSb and metallized with 100 Å of Al. The tunneling current was held constant at 10 nA. Run 1 was over the whole spectral range, and run 2 was for the high voltage region, which is offset for clarity. The spectrum was not averaged. The inset shows the spread in BEEM threshold from a number of runs.

background BEEM current to hundreds of picoamps and rendering the device unsuitable for BEEM spectroscopy. By contrast, sample B was much more resistive because the n-type substrate blocked much of the tunneling current.

Figure 3 shows two BEEM $I-V$ curves from a type B AlSb sample. Each curve was taken from a different place on the sample surface and took approximately 10 s to generate. Since the experiment was carried out in air at room temperature, there was some tip drift even after the system had been given hours to equilibrate. Typical drift rates were about a few nm/min. Hence BEEM scans were not averaged in order to preserve spatial resolution in the experiment. The BEEM $I-V$ curves were analyzed by using the well known Bell–Kaiser model,[9] which assumes that the BEEM threshold behavior takes on the form

$$I_c = \sum_{i=1}^{n} (V - V_i)^2,$$

where I_c is the BEEM collector current, V the tunnel voltage, and V_i the threshold voltage. By examining a large number of runs, it was found that the turn on voltage centered around 1.17 eV with a standard deviation of 0.15 eV. This was in fair agreement with the result obtained by Walachova *et al.*[13] in their study of InAs/AlSb double barrier heterostructures. The BEEM turn on threshold was attributed to the conduction band minimum near the AlSb X point and verified the importance of transport through indirect band minima in AlSb. The L and Γ points of AlSb lie higher and could not be delineated from the BEEM data. As shown in Fig. 3, there was significant variation among the individual BEEM $I-V$ curves. The large variation in individual BEEM thresholds indicated uneveness at the metal–semiconductor interface, consistent with the fact that AlSb barriers are often leaky. This is in contrast with the BEEM study of AlAs, where the BEEM turn on voltage exhibited minimal variation across the wafer.[11]

It should be noted that the BEEM current background noise in the AlSb sample was on the order of 5 pA, which was higher than similarly prepared AlAs samples even through the barrier height in both systems was about 1.2 eV. We attribute this discrepancy to the fact that the background doping was p type for AlSb and n type for AlAs thus the Fermi level and tunneling barriers were likely different even for similar bias voltage. The increased background BEEM current was accounted for by additional hole current in the AlSb system due to the smaller hole barrier. The dominance of hole current was evident in the $I-V$ response of the sample to ambient light.

Background noise was also a significant problem in BEEM spectroscopy of the InAs/AlSb superlattices. This is because the effective superlattice band gap is substantially smaller than that of AlSb, even for samples with a very short period. We have attempted to grow these superlattice structures with period thicknesses of 17, 24, and 48 Å. According to a calculation performed through an eight-band $k \cdot p$ model that included the effects of strain, the band gaps for these structures should be 1.2, 1.15, and 0.88 eV, respectively.[7] The band gaps could be made larger by growing structures with shorter superlattice periods, but the structural quality of the material deteriorated rapidly as the superlattice period

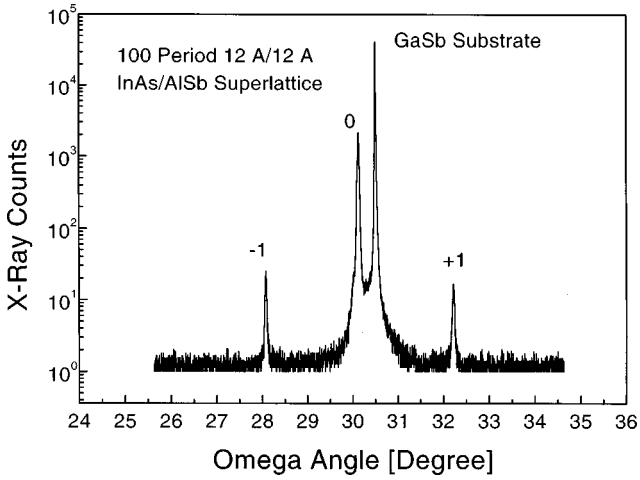

FIG. 4. High resolution x-ray diffraction scan from a 100 period, 12 Å/12 Å/InAs/AlSb superlattice grown on a GaSb substrate.

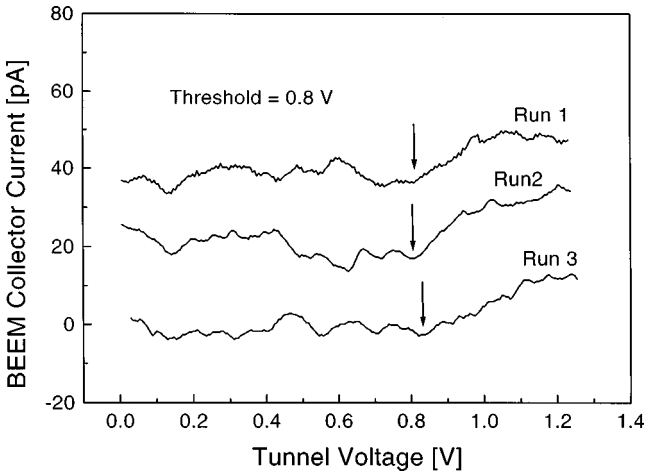

FIG. 6. BEEM $I-V$ curves from the 24 Å period InAs/AlSb superlattice. The superlattice was capped with 50 Å of GaSb and metallized with 100 Å of Au. The samples had previously been stressed by ramping the tip voltage to -3 V while holding the tip current at 50 nA. The tunneling current was held constant at 10 nA during the BEEM scan. The curves were averaged over 255 runs to reduce background noise and are offset for clarity.

was decreased. In fact, x-ray rocking curves for samples with a 17 Å period showed multiple splits at the superlattice peak, indicating that the layer had relaxed from too much strain. The inferior quality of these samples rendered them unsuitable for BEEM studies. The 48 Å longer period sample exhibited good structural integrity but its band gap was too small to keep background BEEM current at a reasonable level. Thus only the 24 Å period samples seemed suitable for BEEM experiments.

Figure 4 shows a high resolution x-ray diffraction scan of the 24 Å period superlattice. The sharp x-ray diffraction satellites were indicative of good structural quality. The $I-V$ curve of the metallized device is shown in Fig. 5 and indicated that the underlying superlattice was n type. The curve deviated significantly from ideal Schottky diode behavior at high voltages. But the low voltage portion of the curve could be used to extract a Schottky barrier height of 0.6 eV.[16]

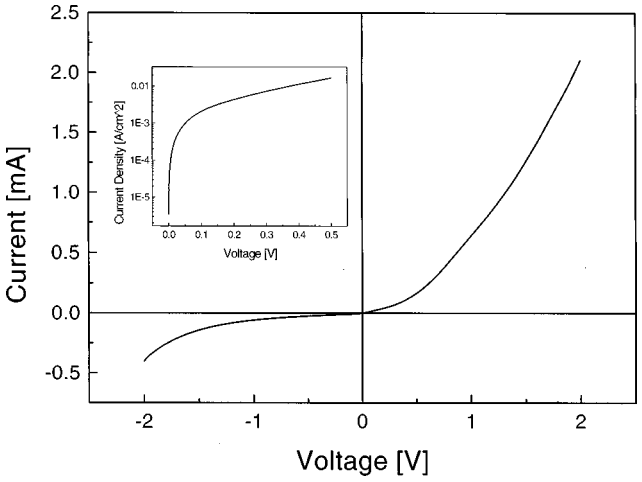

FIG. 5. $I-V$ curve of a BEEM device based on the 24 Å period InAs/AlSb superlattice. Samples were capped with 50 Å of GaSb and metallized with 100 Å of Au. The Au mesa had an area of 1 mm^2. The inset shows a log plot of the current density when the sample was under forward bias, from which a Schottky barrier height of 0.6 eV was extracted.

When these samples were inserted into the BEEM setup, the background BEEM current noise was on the order of 100 pA, which overwhelmed any conventional BEEM signal that would be present. However, it was found that, after the surface was stressed by running a high voltage and current (-3 V and 50 nA) through the STM tip, the metal layer could become deformed resulting in regions where the metal layer was tenuous. When the STM tip was placed over these regions, possible BEEM thresholds could be observed in the BEEM spectroscopy curve. Figure 6 shows some typical BEEM scans after the stress treatment. The estimated possible threshold occurred at around 0.8 eV for the Au/superlattice system and could be reproduced by retracting the STM tip and using it to stress a new region.

IV. SUMMARY AND CONCLUSION

We have demonstrated that BEEM spectroscopy can be applied to the InAs/GaSb/AlSb material system. The Al/AlSb system yielded a BEEM threshold of 1.17 eV, which was attributed to transport through the conduction band minimum near the AlSb X point. The BEEM threshold varied by up to 0.2 eV across the wafer, indicating degradation of the AlSb barrier due to unevenness at the metal–semiconductor interface. It was found that the surface capping layer and the underlying substrate played important roles in suppressing background BEEM current. The junctions formed by InAs/thin AlSb barrier/p-GaSb leaked hole current, which was detrimental to BEEM measurement. In the case of a selectively doped n-type superlattice, BEEM spectroscopy was hampered by considerable background BEEM current. BEEM scans yielded a threshold of 0.8 eV for the Au/24 Å period superlattice system only after considerable stressing of the metal layer. More work would be needed to produce a short period, large band gap superlattice

with superior material quality, the large band gap being needed to suppress background BEEM current.

ACKNOWLEDGMENTS

The authors would like to thank D. H. Chow of Hughes Research Lab for helpful discussions of antimonide growth. This study was supported in part by the Office of Naval Research under Grant No. N00019-89-J-00014 and by the Air Force Office of Scientific Research under Grant No. F49620-93-J-0258.

[1]H. Lee, P. K. York, R. J. Menna, R. U. Martinelli, D. Z. Garbuzov, S. Y. Narayan, and J. C. Connolly, Appl. Phys. Lett. **66**, 1942 (1995).
[2]R. H. Miles, D. H. Chow, Y.-H. Zhang, P. D. Brewer, and R. G. Wilson, Appl. Phys. Lett. **60**, 1921 (1995).
[3]D. H. Chow, R. H. Miles, C. W. Nieh, and T. C. McGill, J. Cryst. Growth **111**, 683 (1991).
[4]D. H. Chow, H. L. Dunlap, W. Williamson, III, S. Enquist, B. K. Gilbert, S. Subramaniam, P.-M. Lei, and G. H. Berstein, IEEE Electron Device Lett. **17**, 69 (1996).
[5]M. Drndic, M. P. Grimshaw, L. J. Cooper, and D. A. Ritchie, Appl. Phys. Lett. **70**, 481 (1997).
[6]M. J. Yang, F.-C. Wang, C. H. Yang, B. R. Bennett, and T. Q. Do, Appl. Phys. Lett. **69**, 85 (1996).
[7]D. H. Chow, Y. H. Zhang, R. H. Miles, and H. L. Dunlap, J. Cryst. Growth **150**, 879 (1995).
[8]W. J. Kaiser and L. D. Bell, Phys. Rev. Lett. **60**, 1406 (1988).
[9]L. D. Bell and W. J. Kaiser, Phys. Rev. Lett. **61**, 2368 (1988).
[10]J. J. O'Shea, T. Sajoto, S. Bhargava, D. Leonard, M. A. Chin, and V. Narayanamurti, J. Vac. Sci. Technol. B **12**, 2625 (1994).
[11]X.-C. Cheng, D. A. Collins, and T. C. McGill, J. Vac. Sci. Technol. A **15**, 2063 (1997).
[12]T. Sajoto, J. J. O'Shea, S. Bhargava, D. Leonard, M. A. Chin, and V. Narayanamurti, Phys. Rev. Lett. **74**, 3427 (1995).
[13]J. Walachova, J. Zelinka, J. Vanis, D. H. H. Chow, J. N. Schulman, S. Karamazov, M. Cukr, P. Zich, J. Kral, and T. C. McGill, Appl. Phys. Lett. **70**, 3588 (1997).
[14]G. Tuttle, H. Kromer, and J. H. English, J. Appl. Phys. **67**, 3032 (1990).
[15]A. A. Talin, D. A. Ohlberg, R. S. Williams, P. Sullivan, I. Koutselas, B. Williams, and K. L. Kavanagh, Appl. Phys. Lett. **62**, 2965 (1993).
[16]S. M. Sze, *Physics of Semiconductor Devices* (Wiley, New York, 1981), p. 279.